

A Neutron Elastic Diffuse Scattering Study of PMN

Guangyong Xu and G. Shirane

Physics Department, Brookhaven National Laboratory, Upton, New York 11973

J. R. D. Copley and P. M. Gehring

NIST Center for Neutron Research, National Institute of Standards and Technology, Gaithersburg, Maryland 20899

(Dated: January 19, 2019)

We have performed elastic diffuse neutron scattering studies on the relaxor $\text{Pb}(\text{Mg}_{1/3}\text{Nb}_{2/3})\text{O}_3$ (PMN). The measured intensity distribution near a (100) Bragg peak in the (hk0) scattering plane assumes the shape of a butterfly with extended intensity in the (110) and ($\bar{1}\bar{1}0$) directions. The temperature dependence of the diffuse scattering shows that both the size of the polar nanoregions (PNR) and the integrated diffuse intensity increase with cooling even for temperatures below the Curie temperature $T_C \sim 213$ K.

PACS numbers: 77.80.-e, 77.84.Dy, 61.12.Ex

I. INTRODUCTION

$\text{Pb}(\text{Mg}_{1/3}\text{Nb}_{2/3})\text{O}_3$ (PMN) is a typical relaxor ferroelectric that has a broad and strongly frequency-dependent dielectric constant. This system has attracted much attention in the last few years, because of the discovery of an ultrahigh piezoelectric response in solid solutions with PbTiO_3 (PT) near the morphotropic phase boundary (MPB)¹. Pure PMN is considered to be a prototype relaxor, and has been studied extensively in recent years². Nevertheless, certain aspects of this system are not fully understood.

Until recently PMN, which remains cubic below the (field-induced) Curie temperature $T_C \approx 213$ K^{3,4}, was believed to exhibit no macroscopic ferroelectric phase transition in zero field. At the same time, x-ray studies of the closely related relaxor $\text{Pb}(\text{Zn}_{1/3}\text{Nb}_{2/3})\text{O}_3$ (PZN) reported a rhombohedral distortion below $T_C \approx 410$ K⁵, and a corresponding ferroelectric phase. However neutron and x-ray studies have now shown that both PMN and PZN retain a cubic structure below T_C ⁶, and that both systems exhibit soft modes at low temperature with identical temperature dependences^{7,8,9}, consistent with that expected for a classical ferroelectric.

Efforts to understand these observations have focused on the polar nanoregions (PNR) present in these relaxor compounds. Burns and Dacol¹⁰ found that on cooling such systems, PNR start to form at temperatures a few hundred degrees above T_C . This temperature was later called the ‘‘Burns Temperature’’ T_d , $T_d \approx 620$ K for PMN. Neutron scattering measurements^{11,12} have demonstrated that diffuse scattering appears in PMN between 600 K and 650 K, consistent with previous optical measurements by Burns and Dacol. The diffuse intensity that develops in relaxors below T_d has been identified with the PNR. Various neutron and x-ray measurements on diffuse scattering have been carried out in order to investigate how PNR are formed, and to determine average sizes and polarizations (atomic shifts) at different temperatures^{13,14,15,16}. Phonon contributions have al-

ways been a potential source of contamination in diffuse scattering measurements. In this paper, we present, and attempt to interpret, elastic diffuse scattering measurements on pure PMN.

II. EXPERIMENT

The experiment was carried out using the Disk Chopper Spectrometer (DCS)¹⁷ at the NIST Center for Neutron Research. The sample was a high quality single crystal of PMN with $\sim 0.1^\circ$ mosaic, and a mass of 3.25 g. A number of neutron scattering studies using this crystal have already been published^{7,8,13,18}. The room temperature lattice parameter is $a = 4.04$ Å. At each of several temperatures, time-of-flight spectra were collected for each of at least 51 successive crystal orientations 0.5° apart using 325 detectors with active dimensions in and normal to the scattering plane of ~ 31 mm and 400 mm respectively. The DCS detectors are located 4000 mm from the sample at scattering angles from 5° to 140° . At an incident neutron wavelength of 5.5 Å, the FWHM (full width at half maximum) of the elastic resolution function was ~ 0.085 meV, and the time between pulses at the sample is 9 ms, effectively eliminating frame overlap. Data were collected near a (100) Bragg peak in the (hk0) scattering plane. The choice of a low Q reflection helps minimize phonon and multiphonon contributions.

III. RESULTS AND DISCUSSION

In Fig. 1, we show the neutron diffuse scattering around a (100) peak in the (hk0) plane measured at different temperatures. Compared with similar x-ray measurements, our neutron scattering measurements have much higher energy resolution, and almost all phonon contributions can be removed by integrating the scattering over an appropriate energy range, 0.075 meV either side of the elastic peak position. In fact, the energy

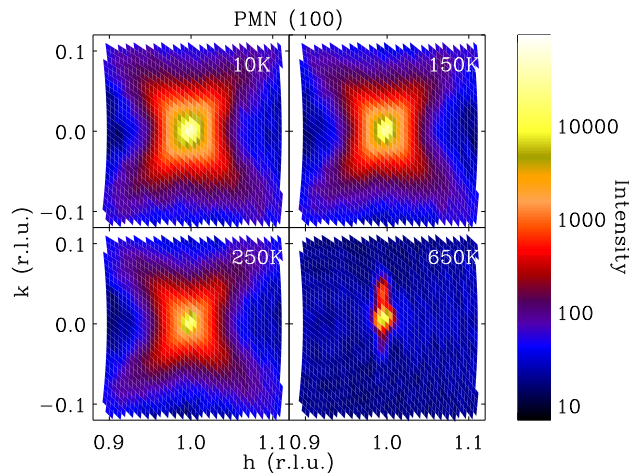


FIG. 1: Logarithmic plots of the neutron elastic diffuse scattering intensity around a (100) Bragg peak, at different temperatures.

spectra show that there is no significant scattering intensity outside this integral range, i.e., phonon contributions are indeed very small around the (100) Bragg peak. The remaining low energy phonon contributions included within this energy integral (phonons with energy transfer $|\hbar\omega| \leq 0.075$ meV) can also be estimated, because phonon intensity increases with temperature, while the elastic diffuse scattering intensity decreases. Since no change in lineshape with temperature was observed, we believe that phonon contributions to the elastic diffuse scattering intensity are negligible.

Comparing the data sets plotted in Fig. 1, one can clearly see that diffuse scattering develops around the (100) peak with decreasing temperature. At ~ 650 K, the “butterfly”-shaped diffuse scattering intensity pattern observed at low temperatures is absent, and only a small trace of intensity transverse to the wave vector $\mathbf{Q} = (1, 0, 0)$ remains. An enlarged plot of the diffuse scattering intensity measured at 200 K is given in Fig. 2. The diffuse scattering intensity has a “butterfly” shape and extends from the Bragg peak along (110) and $(\bar{1}\bar{1}0)$ directions. Previous x-ray diffuse scattering measurements¹⁹ show that the polarizations of the PNR are along $\{111\}$ directions in PMN, and the local symmetry is rhombohedral. This $\{111\}$ type polarization gives the “butterfly” shaped diffuse intensity pattern in the (hk0) plane. The present elastic diffuse scattering results are in good agreement with the x-ray results. Recent neutron diffuse scattering measurements in the (hhk) scattering plane by S.-H. Lee *et al.*²⁰ provide additional evidence to support the $\{111\}$ type polarization in PMN.

Fig. 3 shows cuts through the data along the $(\bar{1}\bar{1}0)$ direction at three selected temperatures. At 400 K, which is well above T_C , the diffuse scattering intensity is already measurable. At higher temperatures, the diffuse scattering intensity becomes even weaker and harder to measure. We use a simple Lorentzian function to describe

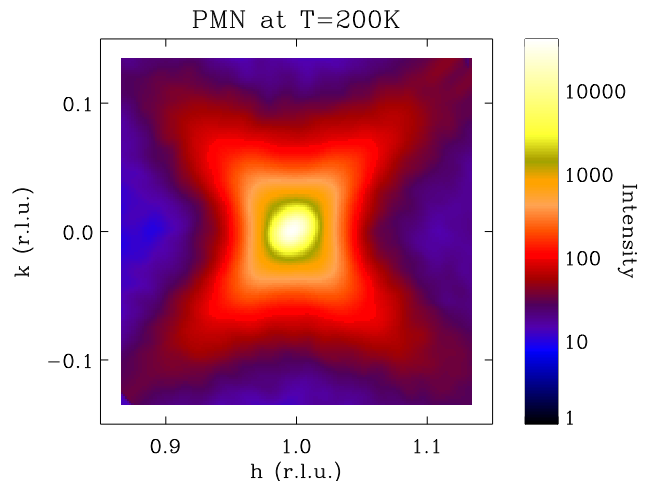


FIG. 2: A smoothed logarithmic plot of the neutron elastic diffuse scattering intensity at 200 K.

the spatial correlation of the atomic displacements contributing to the diffuse scattering:

$$I_{diff} = \frac{I_0 \Gamma}{\pi(q^2 + \Gamma^2)},$$

where I_0 is the integrated diffuse scattering intensity, $\Gamma = 1/\xi$ is the inverse of the real space correlation length ξ , and q is the length of the wave vector measured from the (100) Bragg position. Fig. 3 shows the results of fits to the Lorentzian, plus a Gaussian that describes the central Bragg peak, and a flat background. We have been able to obtain good fits using this model. The fitting parameters are the integrated intensity I_0 and the half width at half maximum Γ of the Lorentzian, the intensity and width of the central Gaussian, and a flat background. I_0 and $\xi = 1/\Gamma$ are plotted in Fig. 4.

In Table. I, we list the integrated diffuse scattering intensity I_0 , correlation length ξ , and the intensity at a selected wave vector $\mathbf{Q} = (1.05, 0.05, 0)$ vs temperature T . The elastic diffuse scattering starts to be noticeable around $T \sim 400$ K, much below $T_d \approx 620$ K. The “correlation length” ξ is a direct measure of the length scale of the static PNR. According to our results, the PNR are small when they first appear at high temperatures, with average sizes around 15 Å (see Fig. 4). Both the spatial correlation length of the atomic displacements and the integrated intensity of the diffuse scattering increase on cooling, even at temperatures below T_C (Fig. 4). At low temperatures the length scale of the PNR reaches ~ 65 Å.

From $T = 300$ K to 100 K, the volume of a single PNR ($V \propto \xi^3$) increases by a factor of ~ 60 , yet the integrated intensity only increases by a factor of ~ 10 . Writing I_0 as the product $N\xi^3|\mathbf{Q} \cdot \delta|^2$, where N is the total number of PNR and δ is the average displacement of atoms within the PNR, we conclude that $N|\mathbf{Q} \cdot \delta|^2$ increases on cooling from high temperatures and then drops dramatically at around T_C , remaining roughly constant below T_C . This

TABLE I: Integrated diffuse scattering intensity I_0 , correlation length ξ , and the intensity at a selected wave vector $Q = (1.05, 0.05, 0)$ vs temperature T.

T (K)	10	100	150	200	250	300	400	500	600
Integrated Intensity I_0	504.9	437.6	361.4	287.1	145.0	59.3	5.62	3.06	-
ξ (\AA)	62.4	64.5	53.8	47.5	19.3	14.6	11.2	13.3	-
$I_{Q=(1.05,0.05,0)}$	174.6	163.7	149.6	137.0	130.2	87.22	20.63	7.90	2.03

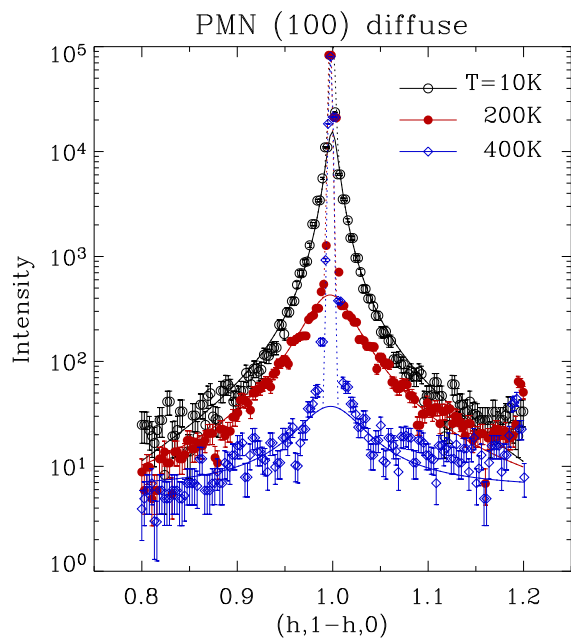


FIG. 3: Diffuse scattering intensities along the (110) direction near the (100) Bragg peak, measured at 10 K, 200 K, and 400 K. The intensity profiles are fitted using a broad Lorentzian function (solid lines), a narrow Gaussian (dashed lines) that describes the resolution-broadened Bragg peak, and a flat background.

is illustrated in Fig. 5 which shows I_0/ξ^3 as a function of T . A likely scenario is that on cooling below T_C , δ remains relatively constant whereas N decreases as the smaller PNR merge together.

Previous inelastic neutron scattering measurements on PMN⁸ have shown that the transverse optic (TO) mode phonon become overdamped near the zone center, starting at $T_d \approx 600$ K, which is roughly the temperature at which the PNR start to appear. We believe that the overdamping of the soft TO mode phonon is directly associated with the formation of the PNR. In other words, the PNR may originate from the condensation of the soft TO mode. Reexamining the neutron diffuse data on PMN by Vakhrushev *et al.*²¹, Hirota *et al.*¹³ have proposed a new interpretation of the atomic displacements derived from the data. The atomic displacements can be decomposed into the sum of two terms with comparable magnitudes: $\delta_{soft} + \delta_{shift}$. δ_{soft} values satisfy the center-of-mass condition and are consistent with the values derived from

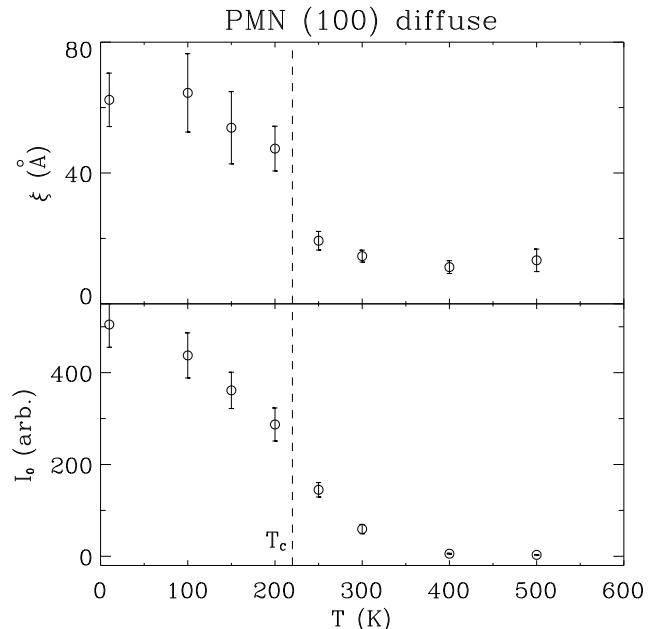


FIG. 4: Top frame: the correlation length ξ as a function of T. Bottom frame: integrated intensity I_0 as a function of T.

inelastic scattering intensities from the soft TO mode. The other term, δ_{shift} , shows that the PNR are shifted along their polar directions relative to the surrounding lattices. This “uniform phase shift” has established convincing connections between the diffuse scattering from the PNR and the condensation of soft TO mode phonons. It is important to note that the magnitude of δ_{shift} is comparable to δ_{soft} , which can be estimated to be around 1/10 of the lattice spacing. This large phase shift creates a huge energy barrier, preventing these polar regions from merging into the surrounding lattices.

Recently, Gehring *et al.* have performed measurements that unambiguously established a true ferroelectric soft mode in PMN⁷. Further inelastic neutron scattering studies by Wakimoto *et al.*⁸ show that the soft mode extends to much lower temperatures below T_C , and that the phonon energy squared $(\hbar\omega_0)^2$, which is inversely proportional to the dielectric constant ϵ , increases linearly with decreasing temperature. These results represent a dynamical signature of a ferroelectric phase below T_C . The phase below T_C is now believed to be the recently discovered phase X^{6,22}, which exhibits an average cubic structure. However, unlike conventional ferroelectric phase

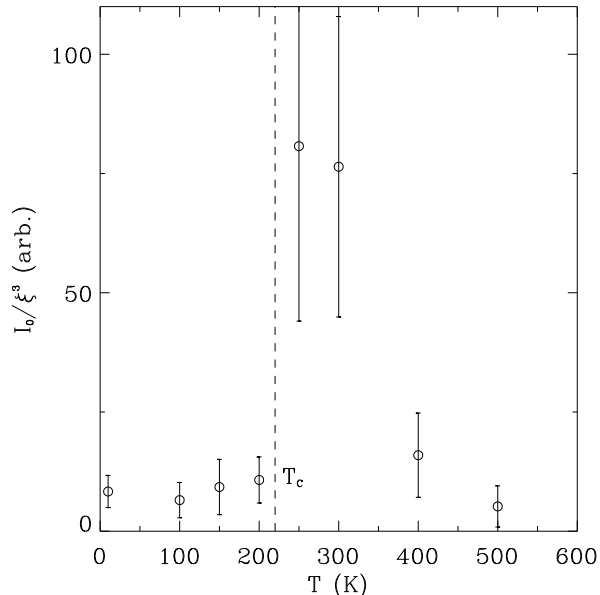


FIG. 5: Plot of I_0/ξ^3 vs T . Parameters were obtained from the fits to the diffuse data.

transitions, no macroscopic (rhombohedral) lattice distortion has been observed. The decoupling of the lattice distortion from the ferroelectric polarization is quite intriguing, and we believe that the interaction between the PNR and the surrounding lattices is the key in solving this puzzle.

Our current understanding of PNR in relaxor systems can be described as follows: At the Burns temperature T_d , the soft TO phonon mode becomes overdamped near the zone center, and starts to condense into PNR. These regions form with local polarizations along $\{111\}$ directions and are shifted uniformly along their individual polarization direction. The number and size of PNR in the system increases with cooling. At the phase transition $T = T_C$, a large scale overall “freezing” of the PNR oc-

curs. Small PNR merge into larger ones and the total volume of PNR in the system keeps increasing. The related ferroelectric soft mode lifetime increases below T_C , and the overdamping near the zone center disappears. A macroscopic ferroelectric polar phase without lattice distortion is then established. Below T_C the size of the PNR can grow slowly with further cooling. However, if the coupling between the PNR and the surrounding lattice is not sufficiently strong, as is the case in pure PMN, then the energy barrier created by the uniform phase shift would prevent the PNR from merging further and forming macroscopic lattice distortions. The resulting phase will have a polar lattice of average cubic structure, but with embedded (rhombohedrally) distorted PNR.

In addition to neutron and x-ray diffuse scattering measurements, recent Raman studies²³ and specific heat measurements²⁴ have also provided useful information on PNR in PMN. We are planning to carry out further diffuse scattering measurements on a series of relaxor systems in the near future.

In summary, we have shown high resolution neutron elastic diffuse scattering data from PMN in the temperature range of 10 K to 650 K. The formation and development of PNR at temperatures above, around, and below T_C have been carefully studied. A merging of smaller PNR into larger ones occurs at the ferroelectric phase transition, while further growth of the PNR into macroscopic rhombohedral domains can not be achieved below T_C .

IV. ACKNOWLEDGMENTS

We would like to thank S.-H. Lee, S. B. Vakhruşev, D. Viehland, and Z.-G. Ye for stimulating discussions. Financial support from the U.S. Department of Energy under contract No. DE-AC02-98CH10886, and the National Science Foundation under Agreement No. DMR-0086210 is also gratefully acknowledged.

¹ S.-E. Park and T. R. Shrout, J. Appl. Phys. **82**, 1804 (1997).

² Z.-G. Ye, Key Engineering Materials **155-156**, 81 (1998).

³ P. Bonneau, P. Garnier, E. Husson, and A. Morell, Mater. Re. Bull **24**, 201 (1989).

⁴ N. de Mathan, E. Husson, G. Calvarin, J. R. Gavarri, A. W. Hewat, and A. Morell, J. Phys. Condens. Matter **3**, 8159 (1991).

⁵ A. Lebon, H. Dammak, G. Calvarin, and I. O. Ahmedou, J. Phys.: Condens. Matter **14**, 7035 (2002).

⁶ G. Xu, Z. Zhong, Y. Bing, Z.-G. Ye, C. Stock, and G. Shirane, Phys. Rev. B **67**, 104102 (2003).

⁷ P. M. Gehring, S. Wakimoto, Z.-G. Ye, and G. Shirane, Phys. Rev. Lett. **87**, 277601 (2001).

⁸ S. Wakimoto, C. Stock, R. J. Birgeneau, Z.-G. Ye,

W. Chen, W. J. L. Buyers, P. M. Gehring, and G. Shirane, Phys. Rev. B **65**, 172105 (2002).

⁹ C. Stock, R. J. Birgeneau, S. Wakimoto, J. Gardner, W. Chen, Z.-G. Ye, and G. Shirane (2002), cond-mat/0301132.

¹⁰ G. Burns and F. H. Dacol, Phys. Rev. B **28**, 2527 (1983).

¹¹ A. Naberezhnov, S. Vakhruşev, B. Doner, D. Strauch, and H. Moudden, Eur. Phys. J. B **11**, 13 (1999).

¹² S. B. Vakhruşev, B. E. Kvyatkovskiy, A. A. Naberezhnov, N. M. Okuneva, and B. Toperverg, Ferroelectrics **90**, 173 (1989).

¹³ K. Hirota, Z.-G. Ye, S. Wakimoto, P. M. Gehring, and G. Shirane, Phys. Rev. B **65**, 104105 (2002).

¹⁴ B. Dkhil, J. M. Kiat, G. Calvarin, G. Baldinozzi, S. B. Vakhruşev, and E. Suard, Phys. Rev. B **65**, 024104

- (2001).
- ¹⁵ H. You and Q. M. Zhang, Phys. Rev. Lett. **79**, 3950 (1997).
- ¹⁶ D. La-Orautapong, J. Toulouse, J. L. Robertson, and Z.-G. Ye, Phys. Rev. B **64**, 212101 (2001).
- ¹⁷ J. R. D. Copley and J. C. Cook, Chem. Phys. **292**, 477 (2003), see also <http://www.ncnr.nist.gov/instruments/dcs>.
- ¹⁸ S. Wakimoto, C. Stock, Z.-G. Ye, W. Chen, P. M. Gehring, and G. Shirane, Phys. Rev. B **66**, 224102 (2002).
- ¹⁹ N. Takesue, Y. Fujii, and H. You, Phys. Rev. B **64**, 184112 (2001).
- ²⁰ S.-H. Lee, P. M. Gehring, and G. Shirane (2003), unpublished.
- ²¹ S. B. Vakhrushev, A. A. Naberezhnov, N. M. Okuneva, and B. N. Savenko, Phys. Solid State **37**, 1993 (1995).
- ²² G. Xu, D. Viehland, J. F. Li, G. Shirane, and P. M. Gehring (2003), cond-mat/0307144.
- ²³ O. Svitelskiy, J. Toulouse, and Z.-G. Ye (2003), cond-mat/0301501.
- ²⁴ Y. Moriya, H. Kawaji, T. Tojo, and T. Atake, Phys. Rev. Lett. **90**, 205901 (2003).